

# Chemically recyclable polyvinyl chloride-like plastics

Received: 21 July 2024

Accepted: 23 September 2024

Published online: 02 October 2024

Xun Zhang, Ximin Feng, Wenqi Guo , Chengjian Zhang  & Xinghong Zhang 

Polyvinyl chloride (PVC) is the world's third-most widely manufactured thermoplastic, but has the lowest recycling rate. The development of PVC-like plastics that can be depolymerized back to monomer contributes to a circular plastic economy, but has not been accessed. Here, we develop a series of chemically recyclable plastics from the reversible copolymerization of cyclic anhydride with chloral. The copolymerization is highly efficient through the anionic or cationic mechanism under mild conditions, yielding polyesters with tunable structure and properties from multiple commercial monomers. Notably, these polyesters manifest mechanical properties comparable to PVC and polystyrene. Meanwhile, such polyesters are flame-retardant like PVC due to high chloride content. Of significance, these polyesters can be depolymerized back to starting monomers at high temperatures owing to the reversibility of the copolymerization, leading to a circular economy. Overall, the readily available monomers, simple synthesis, advantageous performance, and practical recyclability make the polymers promising for applications.

Global plastic production reached a staggering 400.3 million metric tons in 2022<sup>1</sup>. Our lives without plastics would be unrecognizable today<sup>2</sup>. Though society is churning every day to make waste plastics into recycling facilities and recast them as useful items, about 80 wt.% of them end up in landfills and oceans, leading to plastic pollution as among the most pressing current environmental issues<sup>3–6</sup>. An attractive strategy to address the challenge is to use chemically recyclable polymers that can efficiently depolymerize into their starting monomers for repolymerization<sup>7,8</sup>. The last decade has witnessed significant advancement in designed polymers that are convenient for chemical recycling to monomer (CRM)<sup>9–33</sup>. Looking forward, to enable widespread utilization of chemically recyclable polymers in practice, significant achievements will include employing readily available monomers, incorporating useful properties, accessing efficient methods of polymer synthesis, gaining facile processes for CRM, etc.

Polyvinyl chloride (PVC) is the world's third-most broadly produced synthetic thermal plastic, after polyethylene and polypropylene<sup>34</sup>. Global PVC production reaches about 50 million tons per year nowadays. PVC is widely used in the building industry to

produce door/window profiles and also finds use in drinking and wastewater pipes, wire and cable insulation, medical devices, etc. PVC possesses versatile properties such as lightweight, durable, low cost, and easy processability. Flame retardancy is another significant and useful feature that distinguishes PVC from other polyolefins, which is caused by the incorporation of high chlorine content. By contrast, most organic polymer materials are highly flammable, and the fire hazard caused by polymers has always been the main concern of the industry<sup>35</sup>. Additionally, However, compared to other polyolefins, the chemical upcycling of PVC waste is more challenging due to the release of chlorine during its depolymerization, which can deactivate the catalyst<sup>36–40</sup>. Furthermore, PVC is unsuitable for recycling by melt-processing or pyrolysis because of the rapid elimination of harmful hydrochloric acid and other volatiles<sup>36,41</sup>. Nowadays, PVC has the lowest recycling rate among commodity polyolefins. The development of new PVC-like plastics that are capable of CRM is highly attractive, but has not been accessed today as far as we know.

Aliphatic polyesters have been widely regarded as sustainable polymers because of their abundant renewable sources, facile

hydrolytic degradation, and high biocompatibility<sup>42</sup>. Ring-opening polymerization (ROP) of lactone is a versatile method to synthesize polyesters that are capable of CRM<sup>43–45</sup>. Significant progress has been made in this field over the past ten years<sup>46–50</sup>. One of the major limitations in this area is the lack of applicable lactones that can be readily obtained on a large scale. Furthermore, the reported recyclable polyesters usually exhibit unsatisfactory mechanical properties, such as only a handful of recyclable polyesters with a tensile strength of more than 40 MPa<sup>51–53</sup>. Our group recently reported an alternating copolymerization of cyclic anhydride and aldehyde to yield polyesters<sup>54,55</sup>. However, the obtained polyesters possess low molecular weights ( $M_n$ ) of less than 20 kDa and exhibit inadequate mechanical properties. Furthermore, the copolymerization was only achieved through the cationic mechanism and uncontrolled, because the oxygen cation of aldehyde is usually difficult to stabilize.

Here, we for the first time report the reversible copolymerization of chloral with cyclic anhydride to synthesize a series of chemically recyclable PVC-like polyesters (Fig. 1a). Chloral is a low-cost and

commercially available reagent, which is prepared by the reaction of  $\text{Cl}_2$  on ethanol or acetaldehyde (Fig. 1b)<sup>56</sup>. Cyclic anhydride is an easily accessible chemical compound manufactured by heating (bio-based) diacid<sup>57</sup>. In addition, the copolymerization demonstrates the chemical reversibility, enabling the obtained polyesters capable of CRM using  $\text{Sn}(\text{Oct})_2$  as a depolymerization catalyst at high temperatures (180 °C). Meanwhile, the obtained polyesters display favorable mechanical performance comparable to PVC and polystyrene<sup>34,58</sup>. Moreover, the polyesters are flame-retardant like PVC due to high halogen content, suggesting wide application prospects of the polyesters (Fig. 1c).

## Results

Under mild conditions, we tested the copolymerization of chloral with cyclic anhydrides through the anionic and cationic mechanisms, respectively. The bio-derived glutaric anhydride (GA) was first employed as a representative cyclic anhydride<sup>59</sup>. The low-cost  $\text{Et}_3\text{N}$  was used as the catalyst and exhibited high activity toward the anionic copolymerization. With the feeding ratio of  $[\text{chloral}]_0:[\text{GA}]_0:[\text{Et}_3\text{N}] =$

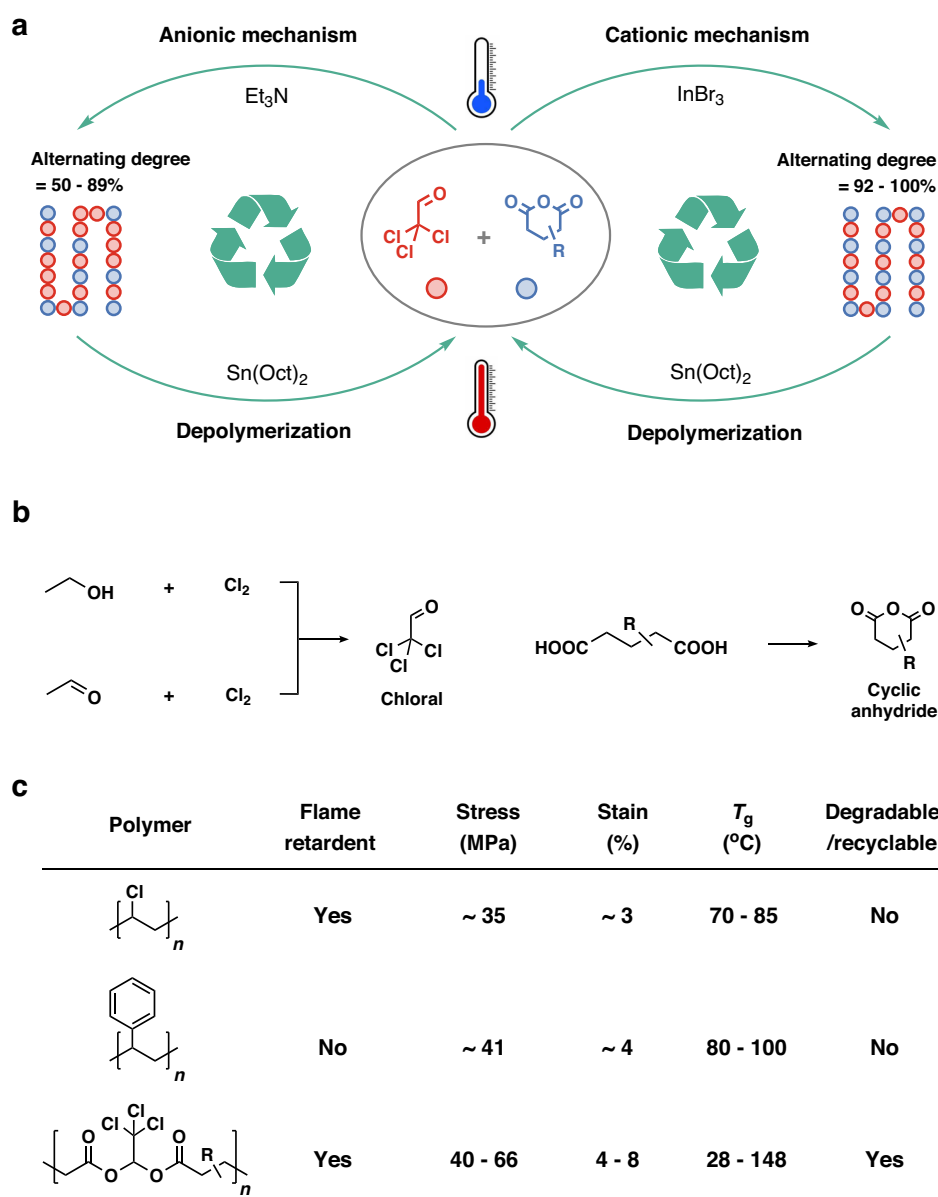


**Fig. 1 | Reversible copolymerization of chloral and cyclic anhydride to yield polyesters that are capable of CRM.** **a**  $\text{Et}_3\text{N}$  and  $\text{InBr}_3$  are used as the catalyst for the anionic and cationic copolymerization, respectively, and  $\text{Sn}(\text{Oct})_2$  is used as a

depolymerization catalyst. **b** The synthesis route of chloral and cyclic anhydride in industry. **c** Compare some of the properties of our polymers with commercial plastics of PVC and polystyrene.

100:100:1, at 25 °C for 15 min, the anionic copolymerization reached a complete monomer conversion, affording the copolymer with a high  $M_n$  of 52.6 kDa and a dispersity ( $\bar{D}$ ) of 1.3 (entry 1 in Table 1). The microstructure information of the obtained polymer was then investigated by  $^1\text{H}$  NMR,  $^{13}\text{C}$  NMR, and  $^1\text{H}$ - $^{13}\text{C}$  HSQC NMR spectroscopy. The  $^1\text{H}$  NMR spectrum shows proton signals at 7.2 ppm attributed to  $\text{C}(=\text{O})\text{OCHOC}(=\text{O})$  (**1**), at 6.6 ppm attributed to  $\text{C}(=\text{O})\text{OCHO}$  (**1'**), at 6.5 ppm attributed to  $\text{OCHO}$  (**1''**), at 2.6 ppm attributed to  $\text{CCH}_2\text{CH}_2$  (**2**), at 2.0 ppm attributed to  $\text{CH}_2\text{CH}_2\text{CH}_2$  (**3**, Fig. 2a and S1a). The  $^{13}\text{C}$  NMR spectrum exhibits carbon signals at 32.8 ppm (**a**), 170.0 ppm (**b**), 171.3 ppm (**b'**), 19.6 ppm (**c**), 90.1 ppm (**d**), 96.4 ppm (**d'**), 96.3 ppm (**d''**), and 96.5 ppm (**e**), respectively (Figure S1b). The proton-carbon relationships of **1** with **d**, **1'** with **d'**, **1''** with **d''**, **2** with **a**, **3** with **c**, are confirmed by the  $^1\text{H}$ - $^{13}\text{C}$  HSQC NMR spectrum (Figure S1c). Hence, the alternating degree (AD) of the obtained polyester is defined as illustrated in Eq. (1),

$$\text{AD} = \frac{A_1 + 1/2A_{1'}}{A_1 + A_{1'} + A_{1''}} \quad (1)$$

where  $A_1$ ,  $A_{1'}$ , and  $A_{1''}$  represent the integral area ratio of **1**, **1'**, and **1''** in the  $^1\text{H}$  NMR spectrum, respectively. Accordingly, the polyester obtained from the  $\text{Et}_3\text{N}$ -catalyzed anionic copolymerization possesses an AD of 66% (entry 1 in Table 1). By contrast, the previously reported copolymerization of cyclic anhydrides with other aldehydes was not achieved through the anionic mechanism<sup>54</sup>.

We then performed the cationic copolymerization of chloral and GA using the commercial Lewis acid of  $\text{InBr}_3$  as a catalyst. With the feeding ratio of  $[\text{chloral}]_0:[\text{GA}]_0:[\text{InBr}_3] = 100:100:1$ , at 25 °C for 47 h (entry 2 in Table 1), the copolymerization reached the chloral monomer conversion of 83%, yielding the polyester with an  $M_n$  of 79.1 kDa, a  $\bar{D}$  of 1.5, and a high AD of 98% (Fig. 2a). Thus, the  $\text{InBr}_3$ -catalyzed cationic copolymerization of chloral and GA exhibited much lower activity than the  $\text{Et}_3\text{N}$ -catalyzed anionic copolymerization. The result is mainly due to the strong inductive effect of chlorine atoms, which makes the aldehyde more reactive by increasing the partial positive charge on the carbonyl carbon. The assumption is also confirmed by the fact that the homopolymerization of chloral can only be achieved through the anionic mechanism and not through the cationic mechanism<sup>60</sup>. Therefore, it is expected that the anionic copolymerization of chloral and GA generates lower AD values than the cationic copolymerization.

For kinetic studies of the  $\text{Et}_3\text{N}$ -catalyzed copolymerization of chloral and GA (Table S1), with the feeding ratio of  $[\text{chloral}]_0:[\text{GA}]_0:[\text{Et}_3\text{N}] = 50:50:1$  and at 25 °C, the decay in the chloral concentration follows first-order kinetics with a high observed rate constant ( $K_{\text{obs}}$ ) of  $0.9 \text{ min}^{-1}$  (Figure S2). During the copolymerization of chloral and GA, the  $M_n$  values of the obtained polyesters are linearly increased with the monomer conversion. In the copolymerization process, the  $\bar{D}$  values of the obtained polyesters remain narrow (1.2–1.4, Figure S3). As the conversion of chloral increased from 19% to >99%, the AD value of the polymer gradually increased from 50% to 66%. The result suggests that under the condition of low monomer concentration, the alternating copolymerization is more advantageous than the chloral homopolymerization. The obtained low- $M_n$  polymer was used for the test of matrix-assisted laser desorption/ionization time-of-flight mass (MALDI-TOF MS), in which multiple distributions were observed (Figure S4). Most of the distributions are attributed to the polyesters bearing dicarboxylate terminals along with few or no chloral-homopolymer linkages. These distributions are proposed to be generated from the initiation of the unavoidable trace amounts of water in the system, which can combine with  $\text{Et}_3\text{N}$  to generate an initiating species of  $[\text{OH}]^+[\text{HEt}_3\text{N}]$  for chain propagation (Figure S5). Due to the low stability of the acetal terminal group, the polymer chain terminals are mainly dominated by carboxylate groups. We also

observed a small amount of distribution with  $\alpha\text{-Et}_3\text{N}$  and  $\omega\text{-COOH}$  terminals from the MALDI-TOF MS, which is believed to be generated from the direct initiation of the nucleophile of  $\text{Et}_3\text{N}$  (Figure S5). Due to the presence of two initiating species of  $\text{H}_2\text{O}$  and  $\text{Et}_3\text{N}$  in the copolymerization system, some of the GPC curves of the copolymers are not standard monomodal.

For kinetic studies of the  $\text{InBr}_3$ -catalyzed copolymerization of chloral and GA (Table S2), with the feeding ratio of  $[\text{chloral}]_0:[\text{GA}]_0:[\text{InBr}_3] = 100:100:1$  and at 25 °C, the decay in the chloral concentration follows first-order kinetics with  $K_{\text{obs}}$  of  $0.041 \text{ h}^{-1}$  (Figure S6). The  $M_n$  values of the obtained polyesters are plausible linearly increased with the chloral conversion, while the  $\bar{D}$  values are in the range of 1.4–1.5 (Figure S7). The MALDI-TOF MS of the low- $M_n$  copolymer displays a main distribution of the polyester with dicarboxylate terminals and complete alternating sequence (Fig. 2b). The trace amounts of water in the system are proposed to act as an initiator in the copolymerization, which can combine with  $\text{InBr}_3$  to generate the initiating species of  $[\text{H}]^+[\text{OHInBr}_3]$  for propagation (Figure S8). The proposed mechanism is consistent with the typical Lewis acid-catalyzed/initiated cationic ROP of cyclic ethers<sup>61</sup>.

We then sought to regulate  $M_n$  of the polyesters by the extra addition of water and 1,4-benzenedimethanol (BDM) to the reaction system (Tables S3 to S6). In the  $\text{Et}_3\text{N}$ -catalyzed copolymerization of chloral and GA, when the water content was increased from 2% to 5%, 8%, 10%, 12%, and 15%, the  $M_n$  of the obtained polyester decreased from 14.3 to 5.9, 4.5, 4.0, 3.2, and 2.5 kDa, while the  $\bar{D}$  values remain narrow (1.1–1.3, Fig. 2c). The  $M_n$  determined by GPC is close to the theoretical  $M_n$ , suggesting a high efficiency of the chain initiation and relatively controlled behavior in the anionic copolymerization. The extra water also reduced the activity of the anionic copolymerization, because the extra water reduces the alkalinity of the system. As an example, the addition of 15% water led to 95% chloral conversion within 24 h (entry 6 in Table S3), while the condition of no extra water achieved >99% chloral conversion within 15 min (entry 1 in Table 1). Additionally, the extra water increased the AD values (from 66% to 81%) of the resulting polymer. We propose that in the anionic copolymerization, the chloral-anion propagating species attacking chloral requires a higher activation energy than attacking cyclic anhydride in kinetics. This hypothesis is confirmed by the experimental results that the resulting copolymers are mainly composed of alternating structure. The extra water reduced the activity of the anionic copolymerization, thus slowing the rate of homo-propagation of chloral relative to cross-propagation to cyclic anhydrides. In the  $\text{InBr}_3$ -catalyzed copolymerization of chloral and GA, when the water content was increased from 2% to 4%, 8%, 10%, 12%, and 15%, the  $M_n$  of the obtained polyester decreased from 31.8 to 17.6, 9.9, 8.2, 6.4, and 5.6 kDa, while the  $\bar{D}$  values were in the range of 1.2–1.5 (Fig. 2d). The  $M_n$  determined by GPC is much higher than theoretical  $M_n$ , indicating a low efficiency of the chain initiation in the cationic copolymerization. The extra water enhanced the activity of the cationic copolymerization, because the extra water increases the amount of initiating species of the system. For instance, the condition of no extra water achieved 83% chloral conversion within 47 h (entry 2 in Table 1), while the addition of 8% water led to 88% chloral conversion within 36 h (entry 3 in Table S4). In the potential high-volume industrial production, due to the inability to strictly control the moisture, there may be large batch differences in the quality of the polymer. The addition of BDM as an initiator to the  $\text{Et}_3\text{N}$ - and  $\text{InBr}_3$ -catalyzed copolymerization also yielded the copolymers with relatively controlled  $M_n$  (Tables S5 and S6, Figures S9 and S10). The reaction activity and the AD,  $M_n$ ,  $\bar{D}$  values of the obtained polymers are similar to the copolymerization system of adding water.

Next, we investigated the impact of polymerization temperature on the copolymerization (Table S7). In the  $\text{Et}_3\text{N}$ -catalyzed copolymerization, when the temperature was increased from 25 °C to 40 °C, 60 °C, 80 °C, and 100 °C, the  $M_n$  of the obtained polyester decreased

**Table 1 | Copolymerization of chloral/bromal with various cyclic anhydrides <sup>a</sup>**

entry	M1	M2	Cat.	T (°C)	t (h)	Conv. (%) <sup>b</sup>	A <sub>1</sub> :A <sub>1</sub> :A <sub>1</sub> :A <sub>1</sub> <sup>c</sup>	AD (%) <sup>d</sup>	M <sub>n</sub> (kDa) <sup>e</sup>	Đ <sup>o</sup>	T <sub>g</sub> (°C) <sup>f</sup>
1	chloral	GA	Et <sub>3</sub> N	25	0.25	>99	56:20:24	66	52.6	1.3	45
2	chloral	GA	InBr <sub>3</sub>	25	47	83	96:4:0	98	79.1	1.5	31
3	chloral	GA	InBr <sub>3</sub>	100	1	69	100:0:0	100	58.6	1.5	28
4	chloral	3-MGA	Et <sub>3</sub> N	25	1.5	93	58:19:23	68	52.4	1.2	41
5	chloral	3-MGA	InBr <sub>3</sub>	25	17	58	88:9:3	93	40.1	1.3	33
6	chloral	3-MGA	InBr <sub>3</sub>	100	1.5	52	100:0:0	100	27.1	1.4	32
7	chloral	DGA	Et <sub>3</sub> N	25	1	94	78:11:11	84	50.4	1.2	75
8	chloral	DGA	InBr <sub>3</sub>	100	12	0	–	–	–	–	–
9	chloral	2,2-DMGA	Et <sub>3</sub> N	25	3	98	72:13:15	79	50.7	1.3	51
10	chloral	2,2-DMGA	InBr <sub>3</sub>	25	26	74	88:7:5	92	26.2	1.4	42
11	chloral	CPDA	Et <sub>3</sub> N	25	6	84	64:20:16	74	37.2	1.1	48
12	chloral	CPDA	InBr <sub>3</sub>	25	119	68	100:0:0	100	13.1	1.5	42
13	chloral	CHDA	Et <sub>3</sub> N	25	24	76	54:29:17	69	44.6	1.1	65
14	chloral	CHDA	InBr <sub>3</sub>	25	215	30	100:0:0	100	13.7	1.4	48
15	chloral	DPA	Et <sub>3</sub> N	60	48	86	100:0:0	100	20.2	1.4	148
16	chloral	DPA	TfOH	60	75	68	100:0:0	100	5.7	1.5	129
17	bromal	GA	Et <sub>3</sub> N	25	48	0	–	–	–	–	–
18	bromal	GA	InBr <sub>3</sub>	25	48	89	91:9:0	95	40.2	1.5	52
19	bromal	3-MGA	InBr <sub>3</sub>	25	48	78	100:0:0	100	31.7	1.5	54
20	bromal	2,2-DMGA	InBr <sub>3</sub>	25	120	87	100:0:0	100	29.0	1.5	50

<sup>a</sup>The copolymerization was performed in CH<sub>2</sub>Cl<sub>2</sub>, [chloral/bromal]<sub>0</sub> = 3.5 M, [cyclic anhydride]<sub>0</sub>: [catalyst] = 100:100:1; <sup>b</sup>Conversion of chloral/bromal, determined by <sup>1</sup>H NMR spectroscopy; <sup>c</sup>Molar ratio of different units in the obtained copolymers, determined by <sup>1</sup>H NMR spectroscopy; <sup>d</sup>Alternating degree of the obtained copolymers; <sup>e</sup>Determined by GPC in THF, calibrated with polystyrene standards (Figures S61–S78); <sup>f</sup>Determined by differential scanning calorimetry (DSC).

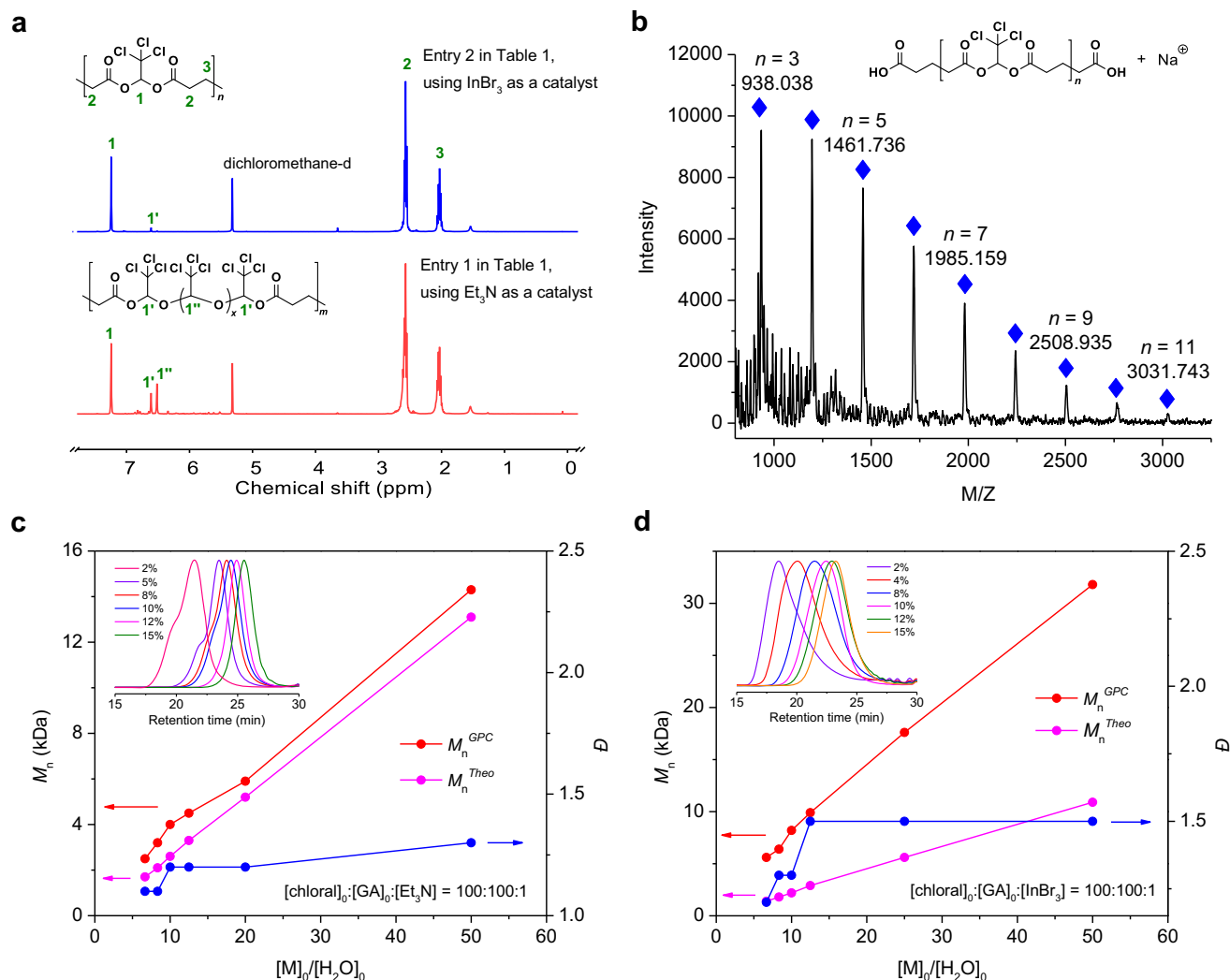


**Fig. 2 | Structure analysis of the obtained polyesters from GA and chloral.** **a** <sup>1</sup>H NMR spectra (400 MHz) of the copolymers in dichloromethane-d (red line: entry 1 in Table 1, using Et<sub>3</sub>N as a catalyst; blue line: entry 2 in Table 1, using InBr<sub>3</sub> as a catalyst). **b** MALDI-TOF MS of low-*M<sub>n</sub>* copolymer (obtained with [chloral]<sub>0</sub>: [GA]<sub>0</sub>: [InBr<sub>3</sub>] = 100:100:1, at 25 °C for 30 min). **c** The relationship of *M<sub>n</sub>*

and *Đ* with the feeding amount of water in the anionic copolymerization, with [chloral]<sub>0</sub>: [GA]<sub>0</sub>: [Et<sub>3</sub>N] = 100:100:1, in Table S3 (insert graph: corresponding GPC curves). **d** The relationship of *M<sub>n</sub>* and *Đ* with the feeding amount of water in the cationic copolymerization, with [chloral]<sub>0</sub>: [GA]<sub>0</sub>: [InBr<sub>3</sub>] = 100:100:1, in Table S4 (insert graph: corresponding GPC curves).

from 52.6 to 30.3, 22.4, 20.5, and 12.2 kDa. The higher temperature might lead to more transesterifications and high initiation efficiency<sup>62</sup>, thus resulting in the decrease of the *M<sub>n</sub>*. Similar results were observed in the InBr<sub>3</sub>-catalyzed copolymerization. When the polymerization temperature was increased from 25 °C to 60 °C and 100 °C, the *M<sub>n</sub>* decreased from 79.1 to 70.2 and 58.6 kDa. Also, the high temperature led to high activity of the cationic copolymerization. As an example, at 100 °C and with the feeding ratio of [chloral]<sub>0</sub>: [GA]<sub>0</sub>: [InBr<sub>3</sub>] = 100:100:1, the chloral conversion was up to 69% within 1 h (entry 3 in Table 1). In addition, by increasing the polymerization temperature, the AD values of the obtained polyesters were increased in both the anionic copolymerization (from 66% to 89%) and the cationic copolymerization (from 96% to 100%). The polyester with complete alternating sequence was obtained at 100 °C from the InBr<sub>3</sub>-catalyzed copolymerization (entry 3 in Table 1, Figure S11). The reason for the increase in AD value at high temperatures may be due to more transesterifications. Taking the anionic copolymerization as an example (Figure S5), when the active species of the carboxyl anion attacks the homopolyacetal unit, the AD value of the polymer will increase. Similar experimental phenomena have also been reported in the copolymerization of formaldehyde and cyclic anhydride<sup>55</sup>.

We also used various bases and acids as catalysts for the copolymerization (Table S8). The commonly used organic bases of 1,8-diazabicyclo[5.4.0]undecane-7-ene (DBU) and 7-methyl-1,5,7-triazabicyclo[4.4.0]dec-5-ene (MTBD) lead to a fast copolymerization. With a feeding ratio of [chloral]<sub>0</sub>: [GA]<sub>0</sub>: [base] = 100:100:1, the anionic copolymerization reached a complete monomer conversion at 25 °C for 6 min, affording the polyesters with AD of 71% (using DBU, entry 1 in Table S8) and 73% (using MTBD, entry 2 in Table S8). The *M<sub>n</sub>* values of 32.1 kDa (using DBU) and 25.9 kDa (using MTBD) are lower than that (52.6 kDa, entry 1 in Table 1) of the polyester obtained by using Et<sub>3</sub>N, while the *Đ* value is higher (1.4 vs. 1.3). The results are mainly caused by DBU (pK<sub>a</sub>: 24.34 in acetonitrile) and MTBD (pK<sub>a</sub>: 25.49 in acetonitrile) having stronger alkalinity than Et<sub>3</sub>N (pK<sub>a</sub>: 18.82 in acetonitrile)<sup>63</sup>, in which a stronger alkalinity can lead to more transesterifications in the anionic copolymerization. Also, more transesterifications lead to higher AD (71% and 73%) relative to the use of Et<sub>3</sub>N (66%, entry 1 in Table 1), consistent with the proposed transesterification mechanism (Figure S5). Additionally, the use of common Brønsted acids of NH(OTf)<sub>2</sub> and TfOH for the cationic copolymerization afforded high-AD (95% and 97%) polyesters with high *M<sub>n</sub>* of 59.5 and 72.8 kDa, respectively (entries 3 and 4 in Table S8).



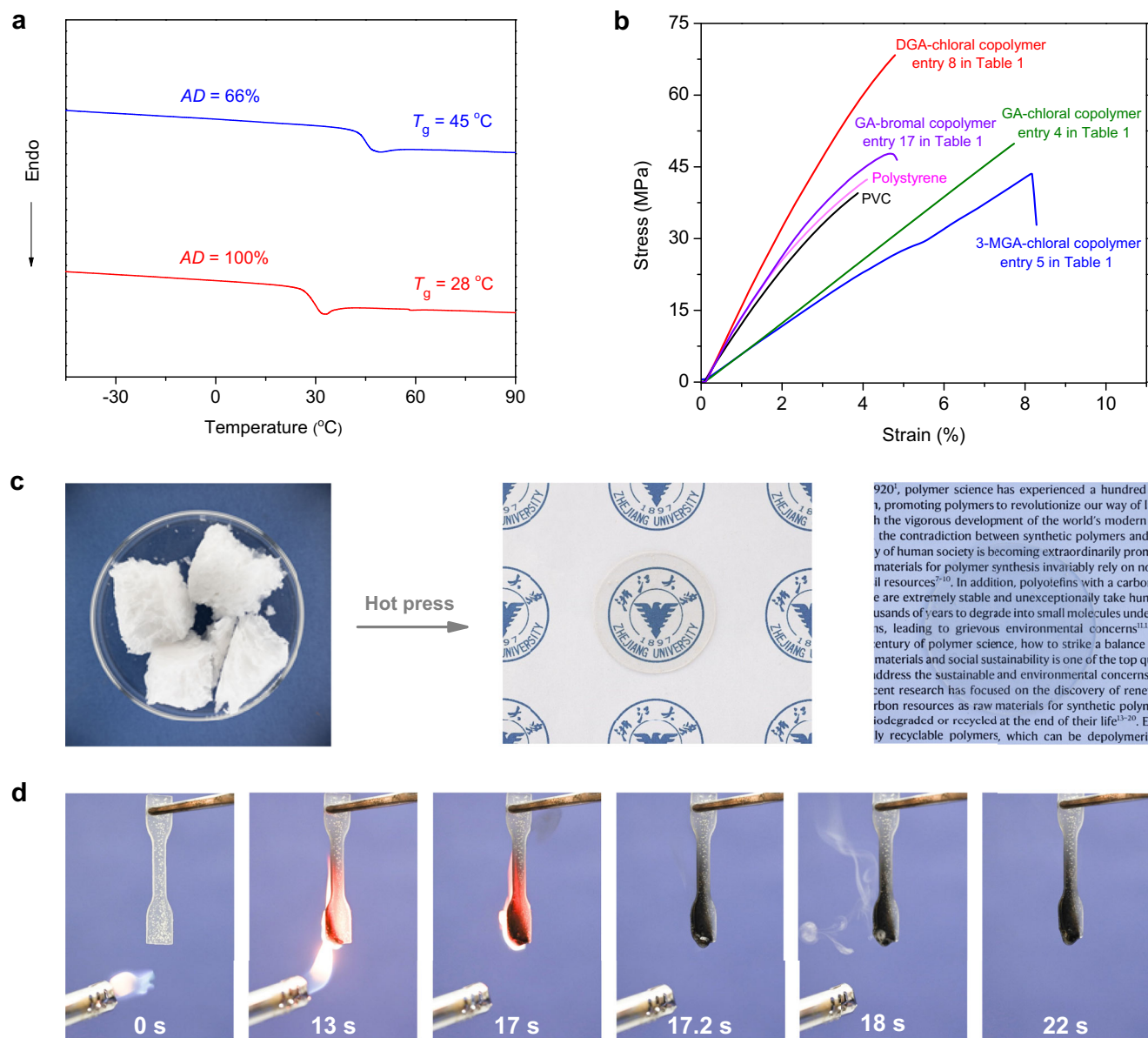


**Fig. 3 | Properties of the obtained halogen-rich polyesters. a** DSC curves of the GA-chloral copolymers (blue line: entry 2 in Table 1; red line: entry 1 in Table 1). **b** stress-strain curves of the obtained polyesters and polystyrene. **c** Photos of the

purified copolymer of GA with chloral, and its wafer made from hot press (diameter: 40 mm; thickness: 1 mm). **d** Photos of the ignited copolymer of GA and chloral (entry 1 in Table 1).

The copolymerization was then successfully extended to bromal and various cyclic anhydrides. Such cyclic anhydrides are commercially available, including 3-methylglutaric anhydride (3-MGA), diglycolic anhydride (DGA), 2,2-dimethylglutaric anhydride (2,2-DMGA), 1,1-cyclopentanediadic anhydride (CPDA), 1,1-cyclohexanediadic anhydride (CHDA), and diphenic anhydride (DPA). Bromal is a commercial reagent and is prepared by the reaction of bromine with ethanol or acetaldehyde.  $\text{Et}_3\text{N}$  and  $\text{InBr}_3$  (TfOH) were used as the catalyst for the anionic and cationic copolymerization, respectively. The anionic copolymerization shows higher activity and generates less content of alternating sequence than the cationic copolymerization. Using such cyclic anhydrides, we obtained several chlorine-rich polyesters with AD of 68%–100%,  $M_n$  of 5.7–52.4 kDa, and  $\bar{D}$  of 1.1–1.5 (entries 4–16 in Table 1, Figures S12–S22). The copolymerization of bromal and cyclic anhydride was realized through the  $\text{InBr}_3$ -catalyzed cationic mechanism, but it was not realized through the  $\text{Et}_3\text{N}$ -catalyzed anionic mechanism (entries 17–20 in Table 1). The results are probably due to the weak inductive effect of the bromine atom, which cannot

stabilize the oxygen anion of the bromal for chain propagation in the anionic copolymerization. At  $25^\circ\text{C}$ , the  $\text{InBr}_3$ -catalyzed copolymerization of bromal and cyclic anhydrides afforded bromine-rich polyesters with high AD of 95%–100%,  $M_n$  of 29.0–40.2 kDa, and  $\bar{D}$  of 1.5 (entries 18–20 in Table 1, Figures S23–S25). Additionally, the diffusion-ordered (DOSY) NMR spectrum of the obtained polymers (entries 1, 11, and 13 in Table 1) manifests a single diffusion coefficient (Figures S26–S28), suggesting only one component of the copolymer rather than the blend of polyaldehyde and the alternating polyester.

We then explored the thermal and mechanical properties of the resulting halogen-rich polyesters. The AD values of the polyester have a huge influence on its glass transition temperatures ( $T_g$ , Fig. 3a, S30, and S32–S46). Generally, the higher the AD value of the polyester, the lower its  $T_g$ . For instance, ignoring the potential impact of  $M_n$ , when the AD is increased from 66% to 74%, 81%, 89%, 96%, and 100%, the  $T_g$  of the copolymer is reduced from  $45^\circ\text{C}$  to  $41^\circ\text{C}$ ,  $38^\circ\text{C}$ ,  $34^\circ\text{C}$ ,  $31^\circ\text{C}$ , and  $28^\circ\text{C}$  (Fig. 3a and S47). Moreover, by changing the substituent group and the halogen atom, the  $T_g$  values of the resulting polyesters are in

the wide range of 28 °C–148 °C. The introduction of halogen atoms enhances the rigidity of the polymer chain and highly increases the  $T_g$  of the polymer, such as the GA-chloral alternating copolymer (entry 3 in Table 1) with a  $T_g$  of 28 °C, while the previously reported GA-acetaldehyde alternating copolymer with a  $T_g$  of −15 °C<sup>54</sup>. Because the volume of the chlorine atom is smaller than that of the bromine atom, the chlorine-substituted polyester have higher chain flexibility than the bromine-substituted polyester, making the free volume discharged faster through the movement of the chain segment. According to the theory of free volume<sup>64</sup>, the chlorine-substituted polyester can only maintain a certain free volume if the chain movement is frozen at a lower temperature relative to the bromine-substituted polyester. Therefore, the  $T_g$  of the bromine-substituted polyester is higher than that of the chlorine-substituted polyester, such as the 3-MGA-chloral alternating copolymer (entry 6 in Table 1) with a  $T_g$  of 32 °C, while the 3-MGA-bromal alternating copolymer with a  $T_g$  of 54 °C (entry 19 in Table 1). These polyesters exhibit  $T_d$  (the temperature at polymer decomposition of 5% in mass fraction) in the range of 173 °C–264 °C, as determined by thermogravimetric analysis (Figures S29–S46). Additionally, we tested the NMR spectra and GPC curves of some copolymers (entries 11 and 15 in Table 1) placed at room temperature for 8 months (Figures S48 and S49). The results suggested that the  $M_n$  of the copolymer did not decrease and no small molecules were released from the copolymers, indicating their relative stability at room temperature. Because of the versatile synthetic method and rich diversity of monomers, the thermal properties of these polymers have an immensely extended range.

Interestingly, many of the obtained polyesters present PVC- and polystyrene-like mechanical properties, as determined by tensile stress-strain curves (Fig. 3a and S50–S55). Similar to PVC, polystyrene is also among the largest plastic commodities in market size (global production per year of more than 15 million tons) with wide applications in packaging, automotive, electronics, etc<sup>58</sup>. The commercial polystyrene samples exhibit the ultimate tensile strength ( $\sigma_B$ ) of 41.0 ± 1.6 MPa and the elongation at break ( $\epsilon_B$ ) of 3.8 ± 0.4% by our measurement, while the commercial pure PVC samples exhibit the  $\sigma_B$  of 35.2 ± 6.4 MPa and the  $\epsilon_B$  of 3.3 ± 0.7%. By contrast, our polyesters exhibit  $\sigma_B$  = 66.1 ± 3.3 MPa and  $\epsilon_B$  = 4.6 ± 0.3% for the DGA-chloral copolymer (entry 7 in Table 1),  $\sigma_B$  = 46.1 ± 2.3 MPa and  $\epsilon_B$  = 4.3 ± 0.8% for the GA-chloral copolymer (entry 1 in Table 1),  $\sigma_B$  = 48.4 ± 2.1 MPa and  $\epsilon_B$  = 7.5 ± 0.3% for the 3-MGA-chloral copolymer (entry 4 in Table 1),  $\sigma_B$  = 40.9 ± 4.2 MPa and  $\epsilon_B$  = 8.0 ± 0.5% for the GA-bromal copolymer (entry 18 in Table 1).

Most of the obtained polyesters are colorless and quite transparent after hot pressing, as shown in Fig. 3c. In particular, the incorporation of large amounts of halogen atoms greatly improves the flame-retardant performance of the polyesters, which is similar to PVC. The ignition experiment of the GA-chloral copolymer is illustrated in Fig. 3d. We first used a lighter to continuously ignite the polyester for 17 seconds. After that, when the lighter was turned off, the flame on the polyester was completely extinguished within 0.2 s, accompanied by the release of a small amount of white smoke. Hence, the excellent flame-retardant performance shows the wide prospects of such polymers in the application of fireproof materials.

We then investigated the thermodynamics of the copolymerization using chloral and GA as monomers (Table S9 and Figure S56).  $\text{InBr}_3$  was used as a catalyst for the copolymerization, because the cationic mechanism led to almost complete alternating copolymerization with  $[\text{GA}] \approx [\text{chloral}]$ . The equilibrium monomer concentration ( $[\text{GA}]_{\text{eq}} \approx [\text{chloral}]_{\text{eq}}$ ) was determined as a function of temperature, i.e., 0.42 M at 80 °C, 0.73 M at 100 °C, 1.33 M at 120 °C, and 2.34 M at 140 °C (Figure S56a). The Van't Hoff plot of  $\ln[\text{GA}]_{\text{eq}}$  versus  $T^{-1}$  provided a straight line with a slope of −4.189 and an intercept of 10.961 (Figure S56b). Then, according to the equation  $\ln[\text{GA}]_{\text{eq}} = \Delta H^\circ/RT - \Delta S^\circ/R$ , the thermodynamic parameters were calculated as  $\Delta H^\circ = -34.8 \text{ kJ mol}^{-1}$

and  $\Delta S^\circ = -91.1 \text{ J mol}^{-1} \text{ K}^{-1}$ . Additionally, based on the equation  $T_c = \Delta H^\circ/(\Delta S^\circ + R \ln[\text{GA}]_0)$ , the  $T_c$  (ceiling temperature) was calculated as 158 °C at  $[\text{GA}]_0 = [\text{chloral}]_0 = 3.5 \text{ M}$  or  $T_c^\circ = 91^\circ\text{C}$  at  $[\text{GA}]_0 = [\text{chloral}]_0 = 1 \text{ M}$ . Therefore, the copolymerization was determined to be chemically reversible.

In view of the reversible character of the copolymerization, we next used the GA-chloral copolymer (entry 1 in Table 1) as an example to examine its closed-loop chemical recycling. In the presence of 2 wt.%  $\text{Sn}(\text{Oct})_2$  as the depolymerization catalyst, a simple distillation operation collected 2.5 g of purified chloral (94% yield) at 180 °C for 4 h (Fig. 4a). Then, by the sublimation of the residue after distillation at 70 °C for 10 h, we obtained 1.2 g of purified GA with 90% yield (Fig. 4b). Both the regenerated chloral and GA have high purity as determined by  $^1\text{H}$  NMR spectra (Fig. 4c, d). Under the same polymerization conditions as entry 1 in Table 1, the copolymerization of the regenerated chloral and GA afforded the copolymer with a similar  $M_n$  and polymer structure to that of the original copolymer (Fig. 4e and S57), thus achieving a circular plastic economy.

By the same method, we also tested the direct recovery of monomers from the GA-chloral copolymer mixed with commercial plastic products and particles, including low-density polyethylene (LDPE), polypropylene (PP), high-density polyethylene (HDPE), PVC, polystyrene (PS), polyethylene glycol terephthalate (PET), polyadipohexylenediamine (PA), and polystyrene-*b*-polybutadiene-*b*-polystyrene (SBS). Using  $\text{Sn}(\text{Oct})_2$  as the depolymerization catalyst, the distillation at 180 °C yielded the crimson liquid containing chloral and pigment additives (Figure S58). The second distillation of the crimson liquid at 100 °C yielded 1.2 g (90% yield) of the purified colorless chloral (Fig. 4f and S59). The sublimation of the solid residue after the first distillation yielded 0.5 g of purified GA with 75% yield (Figure S60). Overall, the chemical recycling of the polyester to monomer is easy to handle.

In conclusion, we have demonstrated the copolymerization of cyclic anhydride with chloral/bromal to yield polyesters that are capable of CRM. Due to the strong inductive effect of chlorine atoms in chloral, the copolymerization of cyclic anhydride with chloral can be achieved through either a cationic or anionic mechanism. Under mild polymerization conditions, the common bases and acids are efficient catalysts for the anionic and cationic copolymerization, respectively. Typically, the anionic copolymerization exhibits higher activity and generates lower AD values than the cationic copolymerization. The method exhibits a high versatility toward several cyclic anhydrides, affording a series of polyesters with tunable structure/performance, AD of 50%–100%, high  $M_n$  of up to 79.1 kDa, and  $T_g$  of 28 °C–148 °C. Interestingly, many of these polyesters manifest PVC- and polystyrene-like mechanical properties. Meanwhile, similar to PVC, these polyesters are flame-retardant due to the incorporation of massive halogen atoms in side chains. Furthermore, the copolymerization is determined to be chemically reversible by kinetic and thermodynamic studies. The chemical recycling of the polyesters to starting monomers with high yield and high purity is realized by simple distillation and sublimation operations using  $\text{Sn}(\text{Oct})_2$  as the catalyst at high temperatures (180 °C). Notably, from the perspective of price, practicality, and versatility, the ambitious goal of our polymers to replace PVC is difficult to achieve at this stage and more systematic research is needed in the future. In general, our findings are expected to furnish graceful guidance for the design of sustainable polymers to meet practical needs.

## Methods

### Materials

Chloral and bromal were purchased from Sigma Aldrich Chemical Co. and were purified by distillation after stirring with calcium hydride for 24 h. The cyclic anhydrides were purchased from Aladdin Reagent Company (Shanghai) and were sublimated twice before use.

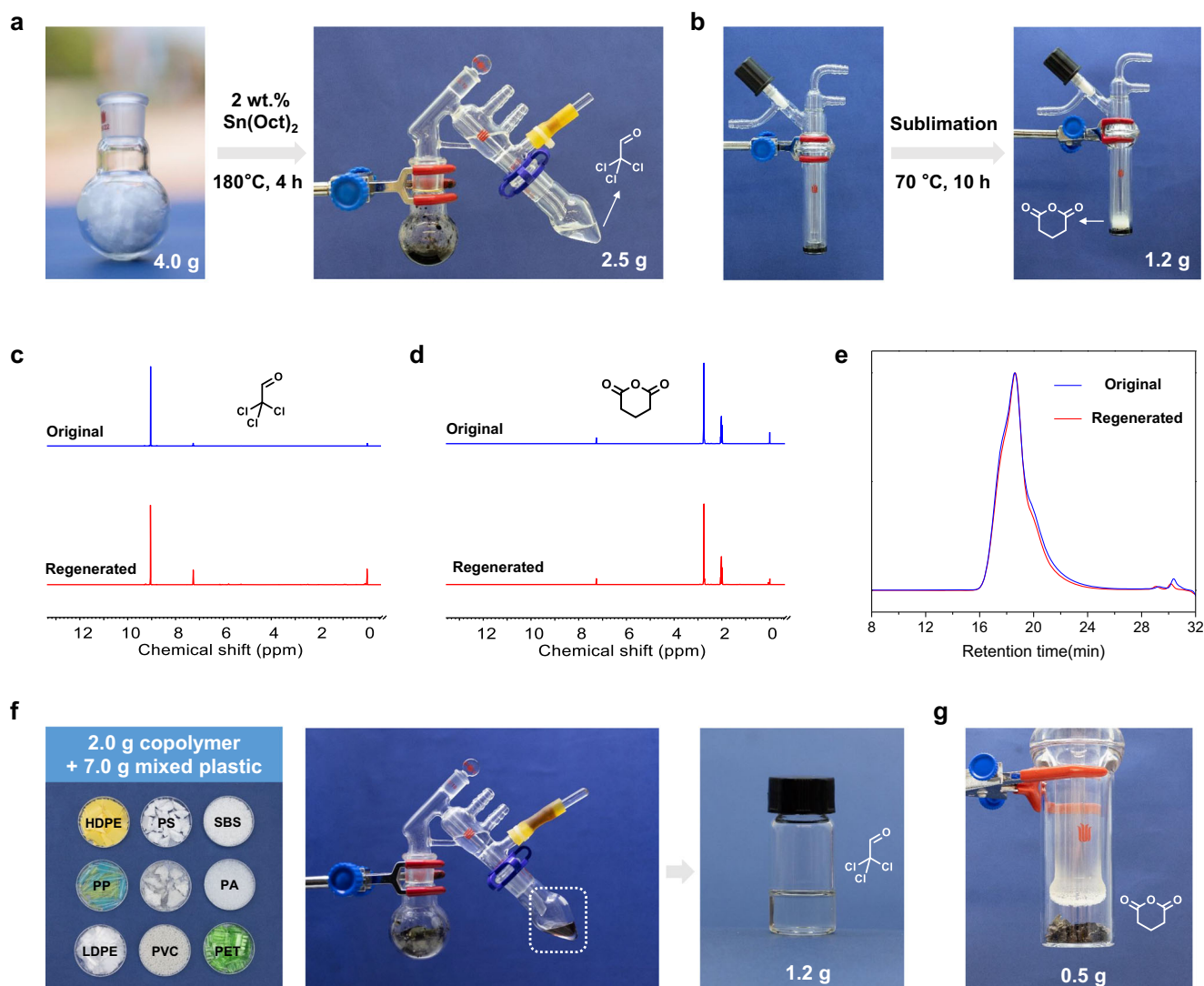


**Fig. 4 | Chemical recycling of the obtained polyesters.** **a** Recovery of chloral by distillation of the copolymer. **b** Recovery of GA from sublimation of the residue after distillation. **c**  $^1\text{H}$  NMR spectra (400 MHz) in  $\text{CDCl}_3$  of the original chloral (blue line) and the regenerated chloral (red line). **d**  $^1\text{H}$  NMR spectra (400 MHz) in  $\text{CDCl}_3$  of

the original GA (blue line) and the regenerated GA (red line). **e** GPC curves of the original copolymer (blue line) and the regenerated copolymer (red line). **f** Recovery of chloral from various mixed common plastics. **g** Recovery of GA by sublimation.

Triethylamine was purchased from Sigma Aldrich Chemical Co. and was purified by distillation after stirring with calcium hydride for 24 h. Catalysts including DBU, MTBD,  $\text{InBr}_3$ ,  $\text{NH}(\text{OTf})_2$ , and  $\text{TfOH}$  were purchased from Sigma Aldrich Chemical Co. and were used as received.

#### Characterization and processing techniques

$^1\text{H}$  and  $^{13}\text{C}$  NMR spectra were performed on a Bruker Advance DMX 400 MHz and chemical shift values were referenced to the signal of the solvent (residual proton resonances for  $^1\text{H}$  NMR spectra, carbon resonances for  $^{13}\text{C}$  NMR spectra).

The molar mass and polydispersity of polymers were measured by GPC at 40 °C using a Waters 1515 isocratic pump, a model 2414 differential refractometer GPC instrument with THF as the mobile phase and Waters Styragel HR3, HR4 and HR5 7.8×300 mm columns. The flow rate of THF was 1.0 mL/min. Linear polystyrene polymers with narrow molar mass distributions were used as standards to calibrate the apparatus.

MALDI-TOF mass spectrometric measurements were performed on a Bruker Ultraflex MALDI TOF mass spectrometer, equipped with a nitrogen laser delivering 3 ns laser pulses at 337 nm. 2,5-

Dihydroxybenzoic acid (DHB) was used as the matrix. Sodium trifluoroacetate was added for ion formation.

The  $T_d$  of the polymers was determined by using TA Q50 instrument. The sample was heated from 40 to 500 °C at a rate of 10 °C/min under nitrogen atmosphere. Temperature when the mass loss is five percent was taken as  $T_d$ .

The DSC measurements of polymers were carried out on a TA Q200 instrument with a heating/cooling rate of 10 °C/min. The sample was heated from -80 to 100 °C under nitrogen atmosphere. Data reported are from second heating cycles.

#### Representative procedure for copolymerization

All copolymerizations were carried out in the glovebox under an Ar atmosphere unless otherwise specified. A 10 mL vial with a magnetic stirrer was first dried in an oven at 110 °C overnight, and then immediately placed into the glovebox. The copolymerization of chloral and cyclic anhydrides described below is taken from entries 1 and 2 in Table 1 as examples.

**For anionic polymerization.**  $\text{CH}_2\text{Cl}_2$  (0.4 mL), glutaric anhydride (4.1 mmol), trichloroacetaldehyde (4.1 mmol), and  $\text{Et}_3\text{N}$  (0.041 mmol)



were added into the reactor. Then, the vial was sealed with a Teflon-lined cap and removed from the glovebox. The reaction mixture was stirred at 25 °C for 15 min. After that, an aliquot portion was then taken from the crude product for determining the composition of the crude products by <sup>1</sup>H NMR spectrum. To obtain purified copolymer, the crude product was dissolved in dichloromethane and then precipitated from an ethanol solution containing hydrochloric acid (2 M). The resulting polymer was dissolved in dichloromethane and then precipitated from ethanol for three times. Finally, the obtained polymer was dried in a vacuum.

**For cationic polymerization.** CH<sub>2</sub>Cl<sub>2</sub> (0.4 ml), glutaric anhydride (4.1 mmol), trichloroacetaldehyde (4.1 mmol), and InBr<sub>3</sub> (0.041 mmol) were added into the reactor. Then, the vial was sealed with a Teflon-lined cap and removed from the glovebox. The reaction mixture was stirred at 25 °C for 47 h. After that, an aliquot portion was then taken from the crude product for determining the composition of the crude products by <sup>1</sup>H NMR spectrum. To obtain purified copolymer, the crude product was dissolved in dichloromethane and then precipitated from an ethanol solution containing sodium phenolate (2 M). The resulting polymer was dissolved in dichloromethane and then precipitated from ethanol for three times. Finally, the obtained polymer was dried in a vacuum.

## Data availability

Data supporting the findings of this study are available within the article (and its Supplementary information files). All other data are available from the corresponding author upon request.

## References

- Nayanathara Thathsarani Pilapitiya, P. G. C. & Ratnayake, A. S. The world of plastic waste: a review. *Clean. Mater.* **11**, 100220 (2024).
- Geyer, R., Jambeck, J. R. & Law, K. L. Production, use, and fate of all plastics ever made. *Sci. Adv.* **3**, e1700782 (2017).
- Korley, L. T. J., Epps, T. H., Helms, B. A. & Ryan, A. J. Toward polymer upcycling-adding value and tackling circularity. *Science* **373**, 66–69 (2021).
- Garcia, J. M. & Robertson, M. L. The future of plastics recycling. *Science* **358**, 870–872 (2017).
- Zhu, Y., Romain, C. & Williams, C. K. Sustainable polymers from renewable resources. *Nature* **540**, 354 (2016).
- Haq, F. M. et al. Defining the macromolecules of tomorrow through synergistic sustainable polymer research. *Chem. Rev.* **122**, 6322–6373 (2022).
- Shi, C., Quinn, E. C., Diment, W. T. & Chen, E. Y. X. Recyclable and (bio)degradable polyesters in a circular plastics economy. *Chem. Rev.* **124**, 4393–4478 (2024).
- Vidal, F. et al. Designing a circular carbon and plastics economy for a sustainable future. *Nature* **626**, 45–57 (2024).
- Jehanno, C. et al. Critical advances and future opportunities in upcycling commodity polymers. *Nature* **603**, 803–814 (2022).
- Abel, B. A., Snyder, R. L. & Coates, G. W. Chemically recyclable thermoplastics from reversible-deactivation polymerization of cyclic acetals. *Science* **373**, 783–789 (2021).
- Arroyave, A. et al. Catalytic chemical recycling of post-consumer polyethylene. *J. Am. Chem. Soc.* **144**, 23280–23285 (2022).
- Si, G. & Chen, C. Cyclic-acyclic monomers metathesis polymerization for the synthesis of degradable thermosets, thermoplastics and elastomers. *Nat. Synth.* **1**, 956–966 (2022).
- Häußler, M., Eck, M., Rothauer, D. & Mecking, S. Closed-loop recycling of polyethylene-like materials. *Nature* **590**, 423–427 (2021).
- Christensen, P. R., Scheuermann, A. M., Loeffler, K. E. & Helms, B. A. Closed-loop recycling of plastics enabled by dynamic covalent diketoenamine bonds. *Nat. Chem.* **11**, 442–448 (2019).
- Wang, Y., Zhu, Y., Lv, W., Wang, X. & Tao, Y. Tough while recyclable plastics enabled by monothiodilactone monomers. *J. Am. Chem. Soc.* **145**, 1877–1885 (2023).
- Yuan, J. et al. 4-Hydroxyproline-derived sustainable polythioesters: controlled ring-opening polymerization, complete recyclability, and facile functionalization. *J. Am. Chem. Soc.* **141**, 4928–4935 (2019).
- Yuan, P., Sun, Y., Xu, X., Luo, Y. & Hong, M. Towards high-performance sustainable polymers via isomerization-driven irreversible ring-opening polymerization of five-membered thionolactones. *Nat. Chem.* **14**, 294 (2022).
- Wu, L. et al. Precision native polysaccharides from living polymerization of anhydrosugars. *Nat. Chem.* **15**, 1276–1284 (2023).
- Rapagnani, R. M., Dunscomb, R. J., Fresh, A. A. & Tonks, I. A. Tunable and recyclable polyesters from CO<sub>2</sub> and butadiene. *Nat. Chem.* **14**, 877–883 (2022).
- Song, Y., He, J., Zhang, Y., Gilsdorf, R. A. & Chen, E. Y. X. Recyclable cyclic bio-based acrylic polymer via pairwise monomer enchainment by a trifunctional Lewis pair. *Nat. Chem.* **15**, 366–376 (2023).
- Sathe, D. et al. Olefin metathesis-based chemically recyclable polymers enabled by fused-ring monomers. *Nat. Chem.* **13**, 743–750 (2021).
- Wang, X. et al. Healable, recyclable, and mechanically tough polyurethane elastomers with exceptional damage tolerance. *Adv. Mater.* **32**, 2005759 (2020).
- Xia, Y., Sun, Y., Liu, Z., Zhang, C. & Zhang, X. Modular alcohol click chemistry enables facile synthesis of recyclable polymers with tunable structure. *Angew. Chem. Int. Ed.* **62**, e202306731 (2023).
- He, C. et al. Polyurethane with β-selenocarbonyl structure enabling the combination of plastic degradation and waste upcycling. *Angew. Chem. Int. Ed.* **63**, e202317558 (2024).
- Zhang, Q., Qu, D.-H., Feringa, B. L. & Tian, H. Disulfide-mediated reversible polymerization toward intrinsically dynamic smart materials. *J. Am. Chem. Soc.* **144**, 2022–2033 (2022).
- Zhang, Z. et al. Strong and tough supramolecular covalent adaptable networks with room-temperature closed-loop recyclability. *Adv. Mater.* **35**, 2208619 (2023).
- Han, X.-W. et al. Circular olefin copolymers made de novo from ethylene and α-olefins. *Nat. Commun.* **15**, 1462 (2024).
- Xu, G. & Wang, Q. Chemically recyclable polymer materials: polymerization and depolymerization cycles. *Green. Chem.* **24**, 2321–2346 (2022).
- Zhao, Y. et al. Chemically recyclable polyolefin-like multiblock polymers. *Science* **382**, 310–314 (2023).
- Zhou, L. et al. Chemically circular, mechanically tough, and melt-processable polyhydroxyalkanoates. *Science* **380**, 64–69 (2023).
- Shieh, P. et al. Cleavable comonomers enable degradable, recyclable thermoset plastics. *Nature* **583**, 542 (2020).
- Qin, B. et al. Closed-loop chemical recycling of cross-linked polymeric materials based on reversible amidation chemistry. *Nat. Commun.* **13**, 7595 (2022).
- Huang, Y.-S., Zhou, Y., Zeng, X., Zhang, D. & Wu, S. Reversible crosslinking of commodity polymers via photocontrolled metal-ligand coordination for high-performance and recyclable thermoset plastics. *Adv. Mater.* **35**, 2305517 (2023).
- Akovi, G.: 2 - Plastic materials: polyvinyl chloride (PVC). In *Toxicity of Building Materials*; Pacheco-Torgal, F., Jalali, S., Fucic, A., Eds.; Woodhead Publishing, 2012; pp 23–53.
- Liu, B.-W., Zhao, H.-B. & Wang, Y.-Z. Advanced flame-retardant methods for polymeric materials. *Adv. Mater.* **34**, 2107905 (2022).
- Jiang, X., Zhu, B. & Zhu, M. An overview on the recycling of waste poly(vinyl chloride). *Green. Chem.* **25**, 6971–7025 (2023).
- Cao, R. et al. Co-upcycling of polyvinyl chloride and polyesters. *Nat. Sustain.* **6**, 1685–1692 (2023).

38. Fagnani, D. E., Kim, D., Camarero, S. I., Alfaro, J. F. & McNeil, A. J. Using waste poly(vinyl chloride) to synthesize chloroarenes by plasticizer-mediated electro(de)chlorination. *Nat. Chem.* **15**, 222–229 (2023).
39. Wang, M. et al. Complete hydrogenolysis of mixed plastic wastes. *Nature Chemical Engineering* 2024, <https://doi.org/10.1038/s44286-024-00064-y>.
40. Zhang, Z. et al. Polyvinyl chloride degradation by a bacterium isolated from the gut of insect larvae. *Nat. Commun.* **13**, 5360 (2022).
41. Jha, R. K. Neyhouse, B. J. Young, M. S. Fagnani, D. E. & McNeil, A. J. Revisiting poly(vinyl chloride) reactivity in the context of chemical recycling. *Chem. Sci.* <https://doi.org/10.1039/D3SC06758K> (2024).
42. Stempfle, F., Ortmann, P. & Mecking, S. Long-chain aliphatic polymers to bridge the gap between semicrystalline polyolefins and traditional polycondensates. *Chem. Rev.* **116**, 4597–4641 (2016).
43. Coates, G. W. & Getzler, Y. D. Y. L. Chemical recycling to monomer for an ideal, circular polymer economy. *Nat. Rev. Mater.* **5**, 501–516 (2020).
44. Tang, X. & Chen, E. Y. X. Toward infinitely recyclable plastics derived from renewable cyclic esters. *Chem* **5**, 284–312 (2019).
45. Li, Z., Shen, Y. & Li, Z. Ring-opening polymerization of lactones to prepare closed-loop recyclable polyesters. *Macromolecules* **57**, 1919–1940 (2024).
46. Hong, M. & Chen, E. Y. X. Completely recyclable biopolymers with linear and cyclic topologies via ring-opening polymerization of gamma-butyrolactone. *Nat. Chem.* **8**, 42–49 (2016).
47. Li, C. et al. Rapid and controlled polymerization of bio-sourced  $\delta$ -caprolactone toward fully recyclable polyesters and thermoplastic elastomers. *Angew. Chem. Int. Ed.* **61**, e202201407 (2022).
48. Zhou, Z., LaPointe, A. M., Shaffer, T. D. & Coates, G. W. Nature-inspired methylated polyhydroxybutyrates from C1 and C4 feedstocks. *Nat. Chem.* **15**, 856–861 (2023).
49. Tu, Y.-M. et al. Biobased high-performance aromatic-aliphatic polyesters with complete recyclability. *J. Am. Chem. Soc.* **143**, 20591–20597 (2021).
50. Li, M.-Q. et al. Ring-opening polymerization of a seven-membered lactone toward a biocompatible, degradable, and recyclable semi-aromatic polyester. *Macromolecules* **56**, 2465–2475 (2023).
51. Zhu, J.-B., Watson, E. M., Tang, J. & Chen, E. Y. X. A synthetic polymer system with repeatable chemical recyclability. *Science* **360**, 398–403 (2018).
52. Fan, H.-Z. et al. Advancing the development of recyclable aromatic polyesters by functionalization and stereocomplexation. *Angew. Chem. Int. Ed.* **61**, e202117639 (2022).
53. Li, X.-L., Clarke, R. W., Jiang, J.-Y., Xu, T.-Q. & Chen, E. Y. X. A circular polyester platform based on simple gem-disubstituted valerolactones. *Nat. Chem.* **15**, 278 (2023).
54. Zhang, X., Guo, W., Zhang, C. & Zhang, X. A recyclable polyester library from reversible alternating copolymerization of aldehyde and cyclic anhydride. *Nat. Commun.* **14**, 5423 (2023).
55. Zhang, X., Xia, Y., Sun, Y., Zhang, C. & Zhang, X. Water-degradable oxygen-rich polymers with AB/ABB units from fast and selective copolymerization. *Angew. Chem. Int. Ed.* **63**, e202315524 (2024).
56. Luknitskii, F. I. Chemistry of chloral. *Chem. Rev.* **75**, 259–289 (1975).
57. Chen, Y., McDaid, P. & Deng, L. Asymmetric alcoholysis of cyclic anhydrides. *Chem. Rev.* **103**, 2965–2984 (2003).
58. Sastri, V. R.: Chapter 6 - Commodity thermoplastics: polyvinyl chloride, polyolefins, and polystyrene. In *Plastics in Medical Devices* (ed. Sastri, V. R) pp 73–119 (William Andrew Publishing: Boston, 2010).
59. Mija, A. et al. Limonene dioxide as a building block for 100% bio-based thermosets. *Green. Chem.* **23**, 9855–9859 (2021).
60. Vogl, O., Miller, H. C. & Sharkey, W. H. Monomer-cast chloral polymers. *Macromolecules* **5**, 658–659 (1972).
61. Kubisa, P.: 4.08 - Cationic ring-opening polymerization of cyclic ethers. In *Polymer Science: A Comprehensive Reference* (ed. Matyjaszewski, K., Möller, M) pp 141–164 (Elsevier: Amsterdam, 2012).
62. Otera, J. Transesterification. *Chem. Rev.* **93**, 1449–1470 (1993).
63. Kaljurand, I. et al. Extension of the self-consistent spectrophotometric basicity scale in acetonitrile to a full span of 28 pKa units: unification of different basicity scales. *J. Org. Chem.* **70**, 1019–1028 (2005).
64. White, R. P. & Lipson, J. E. G. Polymer free volume and its connection to the glass transition. *Macromolecules* **49**, 3987–4007 (2016).

## Acknowledgements

We gratefully acknowledge the financial support of the National Natural Science Foundation of China [52203129 (received by Chengjian Zhang), U23A2083 (received by Xinghong Zhang), and 52373014 (received by Chengjian Zhang)].

## Author contributions

Xun Zhang carried out most of experiments and analysis and wrote the draft. Ximin Feng carried out the analysis of polymerization mechanism. Wenqi Guo carried out the analysis of polymer structure. Chengjian Zhang conceived, designed, and directed the investigation and revised the manuscript. Xinghong Zhang conceived and directed the investigation and revised the manuscript.

## Competing interests

The authors declare no competing interests.

## Additional information

**Supplementary information** The online version contains supplementary material available at <https://doi.org/10.1038/s41467-024-52852-y>.

**Correspondence** and requests for materials should be addressed to Chengjian Zhang or Xinghong Zhang.

**Peer review information** *Nature Communications* thanks the anonymous reviewers for their contribution to the peer review of this work. A peer review file is available.

**Reprints and permissions information** is available at <http://www.nature.com/reprints>

**Publisher's note** Springer Nature remains neutral with regard to jurisdictional claims in published maps and institutional affiliations.

**Open Access** This article is licensed under a Creative Commons Attribution-NonCommercial-NoDerivatives 4.0 International License, which permits any non-commercial use, sharing, distribution and reproduction in any medium or format, as long as you give appropriate credit to the original author(s) and the source, provide a link to the Creative Commons licence, and indicate if you modified the licensed material. You do not have permission under this licence to share adapted material derived from this article or parts of it. The images or other third party material in this article are included in the article's Creative Commons licence, unless indicated otherwise in a credit line to the material. If material is not included in the article's Creative Commons licence and your intended use is not permitted by statutory regulation or exceeds the permitted use, you will need to obtain permission directly from the copyright holder. To view a copy of this licence, visit <http://creativecommons.org/licenses/by-nc-nd/4.0/>.

© The Author(s) 2024